Am J Physiol Gastrointest Liver Physiol 291: G146–G155, 2006.
First published February 16, 2006; doi:10.1152/ajpgi.00003.2006.

Measurement of Ca^{2+} signaling dynamics in exocrine cells with total internal reflection microscopy

Jong Hak Won and David I. Yule

Department of Pharmacology and Physiology, School of Medicine and Dentistry, University of Rochester Medical Center, Rochester, New York

Submitted 5 January 2006; accepted in final form 14 February 2006

Won, Jong Hak, and David I. Yule. Measurement of Ca^{2+} signaling dynamics in exocrine cells with total internal reflection microscopy. *Am J Physiol Gastrointest Liver Physiol* 291: G146–G155, 2006. First published February 16, 2006; doi:10.1152/ajpgi.00003.2006.—In nonexcitable cells, such as exocrine cells from the pancreas and salivary glands, agonist-stimulated Ca^{2+} signals consist of both Ca^{2+} release and Ca^{2+} influx. We have investigated the contribution of these processes to membrane-localized Ca^{2+} signals in pancreatic and parotid acinar cells using total internal reflection fluorescence (TIRF) microscopy (TIRFM). This technique allows imaging with unsurpassed resolution in a limited zone at the interface of the plasma membrane and the coverslip. In TIRFM mode, physiological agonist stimulation resulted in Ca^{2+} oscillations in both pancreas and parotid with qualitatively similar characteristics to those reported using conventional wide-field microscopy (WFM). Because local Ca^{2+} release in the TIRF zone would be expected to saturate the Ca^{2+} indicator (Fluo-4), these data suggest that Ca^{2+} release is occurring some distance from the area subjected to the measurement. When acini were stimulated with supermaximal concentrations of agonists, an initial peak, largely due to Ca^{2+} release, followed by a substantial, maintained plateau phase indicative of Ca^{2+} entry, was observed. The contribution of Ca^{2+} influx and Ca^{2+} release in isolation to these near-plasma membrane Ca^{2+} signals was investigated by using a Ca^{2+} readmission protocol. In the absence of extracellular Ca^{2+}, the profile and magnitude of the initial Ca^{2+} release following stimulation with maximal concentrations of agonist or after SERCA pump inhibition were similar to those obtained with WFM in both pancreas and parotid acini. In contrast, when Ca^{2+} influx was isolated by subsequent Ca^{2+} readmission, the Ca^{2+} signals evoked were more robust than those measured with WFM. Furthermore, in parotid acinar cells, Ca^{2+} readdition often resulted in the apparent saturation of Fluo-4 but not of the low-affinity dye Fluo-4-FF. Interestingly, Ca^{2+} influx as measured by this protocol in parotid acinar cells was substantially greater than that initiated in pancreatic acinar cells. Indeed, robust Ca^{2+} influx was observed in parotid acinar cells even at low physiological concentrations of agonist. These data indicate that TIRFM is a useful tool to monitor agonist-stimulated near-membrane Ca^{2+} signals mediated by Ca^{2+} influx in exocrine acinar cells. In addition, TIRFM reveals that the extent of Ca^{2+} influx in parotid acinar cells is greater than pancreatic acinar cells when compared using identical methodologies.

total internal reflection fluorescence microscopy; Ca^{2+} release; Ca^{2+} influx

EXOCRINE CELLS FROM THE PANCREAS and salivary glands have long served as classic model systems to study agonist-stimulated Ca^{2+} signaling events in nonexcitable cells (1, 2, 25, 44). In these cell types, stimulation with Gαq-linked agonists results in the activation of phospholipase C and the production of inositol 1,4,5-trisphosphate [Ins(1,4,5)P_3], which subsequently triggers Ca^{2+} release from intracellular stores via activation of Ins(1,4,5)P_3 receptors [Ins(1,4,5)P_3R] (6). Ca^{2+} influx across the plasma membrane also accompanies agonist stimulation (5), although the mechanisms that underlie this event are much less well-defined but have been reported to be as a consequence of store depletion (37) and are mediated by a member of the transient receptor potential (TRP) channel family (34) and/or as a result of the activation of a conductance regulated by arachadonic acid following agonist stimulation (26).

Digital imaging of Ca^{2+}-sensitive fluorescent dyes has also established that these Ca^{2+}-signaling events have not only defined temporal but also spatial characteristics, some of which are shared by the two cell types. For example, confocal and wide-field (WF) microscopy (WFM) have demonstrated that the initial Ca^{2+} release events in both pancreas and parotid acinar cells occur in the extreme apical portion of the cell as a result of the almost exclusive expression of Ins(1,4,5)P_3R immediately apposed to the luminal plasma membrane (17, 20, 27, 28, 30, 39, 47). Differences do, however, exist in the propagation of the Ca^{2+} signal away from the initial Ca^{2+} release sites. Specifically, in pancreas, threshold stimulation results in localized Ca^{2+} signals (18), whereas physiological levels of stimulation result in the propagation of a true Ca^{2+} wave toward the basal aspects of the cell (13, 18, 25, 35, 44). In parotid acinar cells, however, agonist stimulation or photolytic release of Ins(1,4,5)P_3 invariably results in large, rapid, global Ca^{2+} signals, even at low stimulus levels (14). These cell type-specific Ca^{2+} signaling characteristics are consistent with the increased expression levels of Ins(1,4,5)P_3R in parotid and the differing distribution in the two cell types of Ca^{2+} clearance machinery; in particular, mitochondria (9, 14, 19, 35, 40). Little, however, is currently known regarding any distinct characteristics or contribution of Ca^{2+} influx pathways in the two cell types. Nevertheless, the particular temporal and spatial aspects of the Ca^{2+} signal in each cell type are entirely consistent with the pivotal role of Ca^{2+} in activating the specific effectors underlying the differing primary physiological processes of each tissue, namely, fluid secretion in parotid and exocytotic secretion from pancreatic acinar cells (25, 44).

Given that both Ca^{2+} release and Ca^{2+} influx occur very close to or at the plasma membrane, a method to monitor Ca^{2+} in this domain has potential to yield insight into these processes with high spatial resolution. Recently, an optical phenomenon termed total internal reflection (TIR) has been successfully exploited to measure near-membrane events (3, 33), including exocytosis/endocytosis in neurons (7) and Ca^{2+} entry through

Address for reprint requests and other correspondence: D. I. Yule, Dept. of Pharmacology and Physiology, School of Medicine and Dentistry, Univ. of Rochester Medical Center, 601 Elmwood Ave., Rochester, NY 14642 (e-mail: david_yule@urmc.rochester.edu).

The costs of publication of this article were defrayed in part by the payment of page charges. The article must therefore be hereby marked "*advertisement*" in accordance with 18 U.S.C. Section 1734 solely to indicate this fact.

voltage-gated Ca^{2+} channels expressed in *Xenopus* oocytes (10, 11). This technique is based on the fact that when light propagating in a dense medium meets a less-dense medium, such as at a glass coverslip and aqueous interface, at a critical angle, all the light is reflected and is termed the TIR. A small fraction of the energy of the light propagates a few hundred nanometers into the aqueous media, and the energy of this so-called "evanescent field" can be absorbed by any fluorophore present. The physical properties of this technique impart resolution in the z-axis, which is unparalleled and not achievable even with techniques such as confocal microscopy.

In the present study, we have used TIR fluorescence (TIRF) microscopy (TIRFM) in pancreatic and parotid acini to monitor near-plasma membrane Ca^{2+} signaling events. These experiments reveal that Ca^{2+} signaling close to the plasma membrane can be measured in a limited area representing contact surfaces between the basal plasma membrane and the coverslip. With the use of experimental paradigms designed to isolate Ca^{2+} release and Ca^{2+} influx, it can be shown that the kinetics of Ca^{2+} signals as measured by TIRFM at physiological concentrations of agonist are not markedly different from those measured with WFM in either pancreatic or parotid acini. These data presumably reflect the fact that the primary process underlying these signals, namely Ca^{2+} release, is occurring at some distance from this contact area. In contrast, when agonist-stimulated Ca^{2+} influx is isolated, TIRFM reveals substantially greater Ca^{2+} influx than WFM and, interestingly, reveals that the magnitude of the fluorescent signal under these conditions is three- to fourfold greater in parotid vs. pancreatic acinar cells.

MATERIALS AND METHODS

Materials. Fluo-4-AM, Fluo-4-FF-AM, Rhod-2-AM, SYTO 16, and rhodamine dextran (100 kDa) were purchased from Molecular Probes. DMEM was purchased from GIBCO. All other materials were obtained from Sigma.

Preparation of pancreatic acini. Mouse pancreatic acini were prepared essentially as described previously (43). Briefly, after CO_2 asphyxiation and cervical dislocation, pancreata were removed from freely fed male National Institutes of Health (NIH)-Swiss mice (25 g). The tissue was enzymatically digested with type-II collagenase in DMEM with 0.1% BSA and 1 mg/ml soybean trypsin inhibitor for 30 min followed by gentle tituration. Acini were then filtered through 100-μm nylon mesh, centrifuged at 75 *g* through 1% BSA in DMEM, and resuspended in 1% BSA in DMEM.

Preparation of parotid acinar cells. Single cells or small clusters of parotid acinar cells were isolated from freshly dissected parotid glands from NIH-Swiss mice (25 g) by sequential digestion with (single cells) or without (cell clusters) trypsin followed by collagenase as previously described (12). After isolation, cells were resuspended in 1% BSA containing Basal Medium Eagle culture media supplemented with 2 mM glutamine, penicillin/streptomycin, incubated at 37°C, and gassed with 5% CO_2 and 95% O_2 until ready for use.

Imaging. Before experimentation, aliquots of cell suspensions from pancreas or parotid were loaded by incubation with either 4 μM Fluo-4-AM or Fluo-4-FF-AM as indicated in a HEPES-buffered physiological saline solution (HEPES-PSS) containing (in mM) 5.5 glucose, 137 NaCl, 0.56 $MgCl_2$, 4.7 KCl, 1 Na_2HPO_4, 10 HEPES (pH 7.4), and 1.2 $CaCl_2$, after which they were resuspended in HEPES-PSS and kept at 4°C until ready for use. Before experiments, acini were seeded on coverslips that formed the base of a superfusion chamber and were mounted on the stage of an Olympus IX71 inverted microscope. Solution changes were accomplished by selecting flow from a multichambered, valve-controlled, gravity-fed reservoir.

Excitation light was provided by a 20 mW Argon Krypton laser (Omnichrome 43 series; Melles Griot, Carlsbad, CA). The laser was directed through a light guide into an Olympus TIRF illuminator attached to the rear port of the microscope and through appropriate filters to select individual laser lines to a TIRF-optimized high-numerical aperture (NA) oil-immersion objective (Olympus Plan APO ×60, 1.45 NA). Excitation of Fluo-4 or Fluo-4-FF by the 488-nm line of the laser was accomplished by using a 488 band-pass filter (BP, 10 nm), 500-nm dichroic beam splitter, and emitted light was collected through a 524 (BP, 50 nm) band-pass filter. Changes in Fluo-4 fluorescence are expressed as $\Delta F/F_0$, where F is the fluorescence captured at a particular time, and F_0 is the mean of the initial 10 fluorescence images captured. Excitation using the 568-nm laser line was accomplished using a 568 band-pass filter (BP 10 nm), 590-nm dichroic beam splitter, and 600-nm long-pass emission filter (Chroma technology, Battleboro, VT). Images were collected every 200 ms using a Cooke Sensicam QE camera controlled by INDEC Biosystems Imaging Workbench software. For WFM imaging, minimal laser power was used, and the beam focused on the back plane of the objective. For TIRFM, the laser was set to 50% power, and the angle of the beam was controlled within the objective lens by means of a translation stage incorporated into the illuminator and controlled manually by a micrometer. TIR was judged to have occurred based on the criteria established in Fig. 1; that during TIRF, intracellular fluorescence did not substantially overlap with excitation by the evanescent wave of extracellular dye. In addition, settings for TIRFM using the 488-nm laser line were verified by imaging 200-nm polystyrene beads coated with fluorescent dye; TIR was judged to be occurring when discrete fluorescence of stationary, adhered beads ("landmark" beads) plus the occasional random "flashes" of beads transiently settling on the coverglass were observed. The focus did not appreciably change over a 10-min observation period, as judged by the fluorescence from landmark beads.

Statistical analysis. Data are presented as means ± SE. Experimental groups were compared using a nonpaired Student's *t*-test or Mann-Whitney test.

RESULTS

Establishing conditions for TIR microscopy. Initial experiments were performed to establish reproducible parameters that could be considered as indicative of TIRFM in exocrine acinar cells. After resuspension in HEPES-PSS containing rhodamine-conjugated dextran (100 μM), small acini (3–8 cells, as judged by nuclear staining) were seeded onto clean coverslips and allowed to attach for ~10 min. Experiments were generally not performed in single cells, because in the absence of junctional complexes, the cells did not adhere firmly enough to the coverglass to allow the necessary stationary measurement with any regularity. In some early experiments, the coverslips were coated with the extracellular matrix protein fibronectin (10 μg/ml) before seeding acinar cells. This maneuver, however, did not markedly alter the morphology of the cells as visualized by WF or TIRF illumination and, in the majority of experiments, was not continued. WF excitation at 488 nm resulted in essentially homogeneous fluorescence representing cytoplasmic Fluo-4 fluorescence as shown for the representative pancreatic acinus in Fig. 1, *A* and *B*. As the incident angle of the laser beam was adjusted, cytoplasmic fluorescence was rapidly lost, and at the point TIR was achieved, only small patches of fluorescence could be observed as shown in Fig. 1*C* and the *overlay* in Fig. 1*F*. This fluorescence presumably represents points of adherence between the

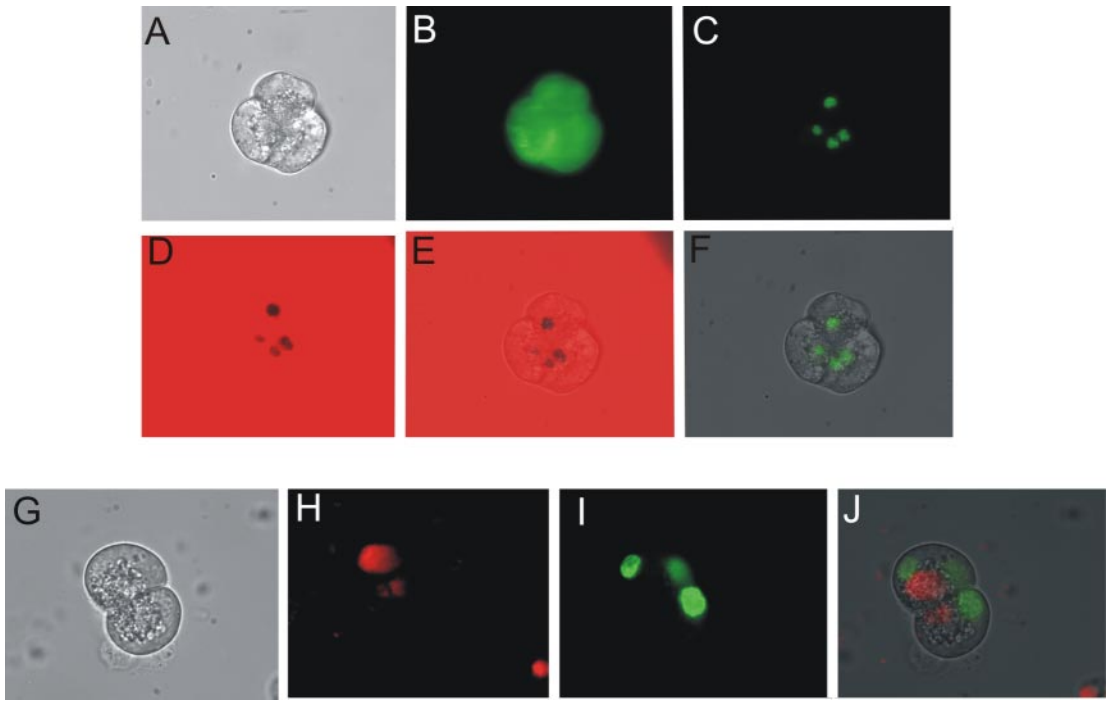

Fig. 1. Establishing total internal reflection fluorescence microscopy (TIRFM) excitation in exocrine cells. *A*: bright-field image of a small pancreatic acinus, prepared as described in MATERIALS AND METHODS. In *B*, the acinus depicted in *A* was loaded with fluo-4 (4 μM), and the dye was excited using the 488-nm argon-krypton laser line in wide-field mode (WFM). In *C*, the dye was excited following total internal reflection of the incident excitation light. In *D*, rhodamine-dextran (100 μM) in the external solution was excited using TIRFM with the 568-nm laser line. *E*: overlay images of *A*, *C*, and *D*. *F*: overlay image of *A* and *C*. *G*: bright-field image of a doublet of pancreatic acinar cells. *H*: TIRFM of cells shown in *G* following rhod-2 loading. *I*: staining of nuclei with SYTO 16 (1 μM) in WFM. *J*: overlay image of *G*, *H*, and *I*.

acinar cell plasma membrane and the coverslip. This contention was further strengthened by the observation that 568-nm TIRF excitation of rhodamine dextran in the extracellular medium resulted in fluorescence that was excluded from areas excited by 488-nm TIRF illumination of Fluo-4 as shown in Fig. 1*D* and the *overlay* in 1*E*. These data are consistent with the extracellular rhodamine dextran being in the bulk solution and thus largely excluded from areas of contact between the cell and coverslip. The region of the acinar cell amenable to TIRF illumination did not substantially overlap with the basolateral volume of the cell containing the nucleus as demonstrated in Fig. 1*H*, which shows 568-nm TIRF illumination of a Rhod-2-loaded small acinus and subsequent 488-nm WF illumination of SYTO 16 nuclear stain (Fig. 1*I* and *overlay* in Fig. 1*J*). These experiments were repeated in four preparations of pancreatic acinar cells and three parotid acinar cell preparations. Taken together, these data indicate that the TIRF illumination appears to exclusively excite intracellular dye in a limited region distal from the basal plasma membrane and encompassing the apical one-third of the acinar cell.

Measurement of agonist-stimulated Ca^{2+} signals in pancreatic and parotid acinar cells with TIRFM. Experiments were first performed measuring intracellular Ca^{2+} concentration $\{[Ca^{2+}]_i\}$ using TIRFM under conditions established in Fig. 1. Images were acquired every 0.5–1 s, and the images were collected and stored to memory. The average gray value from within a polygon corresponding to the original area of TIRF was used to generate line profiles of the stimulated changes in $[Ca^{2+}]_i$. An example of a series of images and the line profile is shown in Fig. 2 for a small pancreatic acinus incubated with ionomycin and shows that the evoked fluorescence changes, unlike in WFM, occur within the specific region subjected to TIRFM and, importantly, that the area subjected to TIRFM does not markedly change/expand during the experiment.

Agonist stimulation of both pancreatic and parotid acinar cells results in stereotypical Ca^{2+} signals with defined temporal and spatial characteristic properties that depend largely on the concentration of agonist (36, 42, 46). To gain insight into the characteristics of near-plasma membrane Ca^{2+} signals in acinar cells, experiments were performed to compare the characteristics of Ca^{2+} signals observed with TIRFM with those reported for globally averaged Ca^{2+} signals using WFM. Fluo-4-loaded acinar cells were stimulated with either low concentrations (100–300 nM) of the muscarinic agonist CCh, considered to stimulate a physiological-type Ca^{2+} signal, or supermaximal CCh concentrations (10 μM), and $[Ca^{2+}]_i$ was measured using TIRFM. These concentrations of agonists were chosen to represent approximately equivalent concentrations in terms of activation of physiological end points in the respective cell types. As shown in Fig. 3, *A* and *B*, for parotid and pancreas acinar cells, respectively, stimulation with 300 nM CCh resulted in Ca^{2+} oscillations with characteristics very similar to those reported previously for WFM; typically, stimulation resulted in repetitive sinusoidal oscillations that are generally thought of as primarily the result of repetitive Ca^{2+} release and subsequent clearance. These transients were superimposed on an elevated baseline with a period between 4 and 12 cycles per minute (8, 46). Given the K_d of Fluo-4 for Ca^{2+} [~1 μM in situ (38)], this observation is unexpected if the sites of Ca^{2+} release or influx are localized in close proximity to the

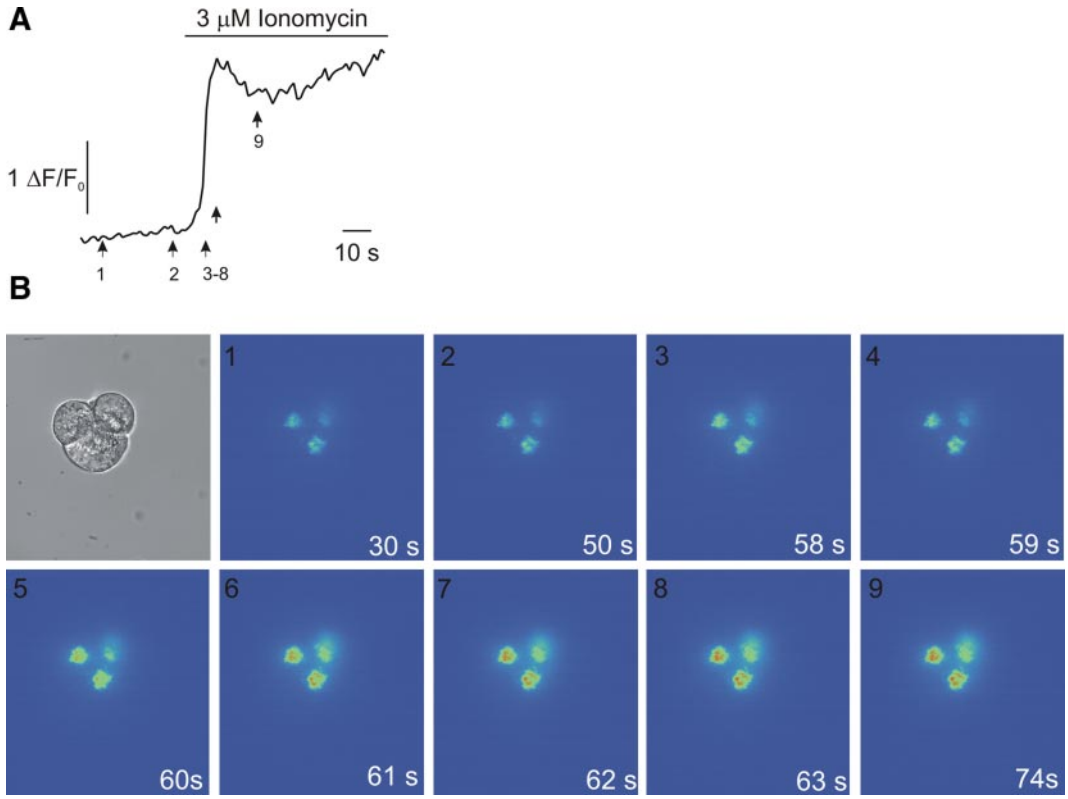

Fig. 2. Ca^{2+} measurement using TIRFM. Under conditions established in Fig. 1, intracellular Ca^{2+} {$[Ca^{2+}]_i$} was measured using TIRFM. *A*: line profile of average fluorescence in a polygon corresponding to the original region subject to TIRFM. *B*: series of images obtained from a small pancreatic acinus at the time points indicated in *A*. ΔF/F0, changes in Fluo-4 fluorescence.

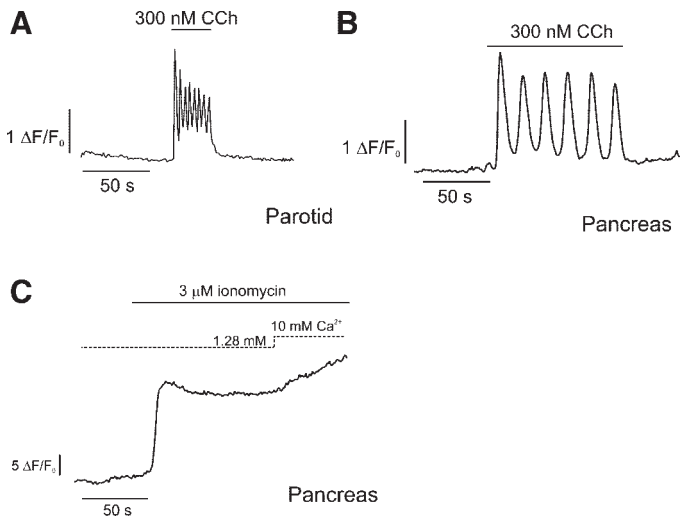

Fig. 3. Measurement of $[Ca^{2+}]_i$ using TIRFM following physiological agonist stimulation. *A*: representative trace from a Fluo-4-loaded (4 μM) parotid acinus using TIRFM. Stimulation with a physiological concentration of agonist results in oscillations of fluorescent signal, indicative of oscillating $[Ca^{2+}]_i$ levels. *B*: similar experiment performed in pancreatic acinar cells. The Ca^{2+} oscillations in parotid were qualitatively similar to those observed in pancreatic acinar cells but of higher frequency as previously reported. *C*: representative trace of a pancreatic acinus incubated with ionomycin. The Ca^{2+} signal is of greater magnitude (note difference in scale bars), and the signal appears close to saturation as increasing Ca^{2+} in the external bath did not further markedly increase the signal.

volume of dye subjected to TIRFM, because the dye would be predicted to be saturated in close proximity to Ca^{2+} channels. Thus these data suggest that, under these conditions, the Ca^{2+} signal is generated at a site distant from the area that can be monitored with TIRFM. To support this idea and to confirm that TIRFM in acinar cells is capable of measuring localized Ca^{2+} signals, acini were treated with ionomycin to allow the transport of Ca^{2+}, presumably in a uniform manner, across the plasma membrane. As shown in Fig. 3*C*, $[Ca^{2+}]_i$ rapidly increased, and the fluorescence of Fluo-4 appeared saturated as indicated by little further increase in fluorescence when extracellular Ca^{2+} was increased from 1.28 to 10 mM. These data are consistent with the ability of TIRFM to measure localized subplasma membrane $[Ca^{2+}]$ changes and also indicate that the area of the cells subjected to TIRFM is unlikely to represent an area of restricted access to the extracellular plasma membrane.

Next, acinar cells were stimulated with supermaximal concentrations of agonist, which would be expected to result in maximal Ca^{2+} release followed by store depletion-gated Ca^{2+} influx. Stimulation with supermaximal concentrations of CCh (10 μM) resulted in a rapid initial peak response followed by a plateau phase, which was maintained during agonist stimulation (Fig. 4, *A* and *B*; for parotid and pancreas, respectively). This pattern of response appeared qualitatively similar to that reported for experiments using WFM, although the plateau phase, of the response, indicative of Ca^{2+} influx, appeared more substantial compared with that previously reported in the literature (see Refs. 41 and 45; see also Fig. 5, *A* and *B*, for a comparison of WFM and TIRFM). These data suggest that

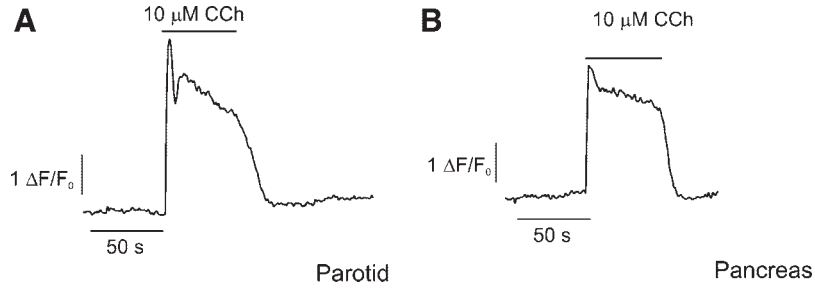

Fig. 4. Measurement of $[Ca^{2+}]_i$ using TIRFM following maximal agonist stimulation. *A*: representative trace from a Fluo-4-loaded (4 μM) parotid acinus using TIRFM stimulated with a supermaximal concentration of agonist. *B*: similar experiment is shown, which was performed in pancreatic acinar cells. In each cell type, a rapid initial peak in the Ca^{2+} signal was evoked followed by a substantial plateau that was maintained while the stimulus was present.

TIRFM may provide a useful measurement of localized Ca^{2+} influx under some conditions. Therefore, subsequent experiments were designed to investigate this more thoroughly by isolating Ca^{2+} release and Ca^{2+} influx.

Measurement of isolated agonist-induced Ca^{2+} release and Ca^{2+} influx with TIRFM in parotid acini. To further investigate the properties of agonist-stimulated Ca^{2+} signals using TIRFM, Ca^{2+} release and Ca^{2+} influx were isolated. A Ca^{2+}-readdition paradigm was used, whereby pancreatic and parotid and acinar cells were initially stimulated in the absence of extracellular Ca^{2+} followed by readmission of Ca^{2+} to the extracellular bathing media. The changes in fluorescence were monitored using TIRFM or WFM. As shown in Fig. 5*A*, in parotid acinar cells, stimulation in the absence of extracellular Ca^{2+} resulted in a rapid increase in $[Ca^{2+}]_i$, which subsequently decayed to prestimulus levels in ~2 min. The profile or magnitude of the response was not statistically different when measured with TIRFM or WFM [6.25 ± 0.35 (n = 13) vs. 4.96 ± 0.19 (n = 3) ΔF units, t-test $P > 0.05$, TIRFM (Fig. 5*A*) vs. WFM (Fig. 5*B*), respectively; see Fig. 8*A* for summary], again consistent with the sites of Ca^{2+} release occurring some distance from the area subjected to TIRFM. In contrast, on readmission of extracellular Ca^{2+}, the fluorescence signal was statistically significantly greater when measured with TIRFM than when measured using WFM [14.9 ± 1.52 (n = 13) vs. 1.72 ± 0.311 (n = 3) ΔF units, t-test $P < 0.01$; TIRFM (Fig. 5*A*) vs. WFM (Fig. 5*B*), respectively; see Fig. 8*A* for summary]. The signal appeared to be largely saturated in the TIRFM experiments, because increasing external Ca^{2+} from 1.28 to 10 mM did not substantially increase this signal further as shown in Fig. 5*A*. The increase in $[Ca^{2+}]_i$ following readmission of extracellular Ca^{2+} was unaffected by preincubation of the cells with 100 μM ryanodine [12.05 ± 1.77 ΔF units (n = 6)], indicating that Ca^{2+}-induced Ca^{2+} release (CICR) through ryanodine receptors was unlikely to underlie this observation. When similar TIRFM experiments were performed in cells loaded with the low-affinity indicator Fluo-4-FF, increasing external Ca^{2+} from 1.28 to 10 mM following stimulation with 10 μM CCh resulted in a further increase in fluorescence as shown in Fig. 5*C*, indicating that this dye was unlikely to be saturated under these conditions. These data indicate that TIRFM reveals elevations in $[Ca^{2+}]_i$ of substantially greater magnitude than with conventional WFM. These Ca^{2+} signals presumably represent substantial Ca^{2+} influx occurring locally at the plasma membrane.

At least at supramaximal concentrations of agonists, it is widely believed that depletion of intracellular Ca^{2+} pools is a

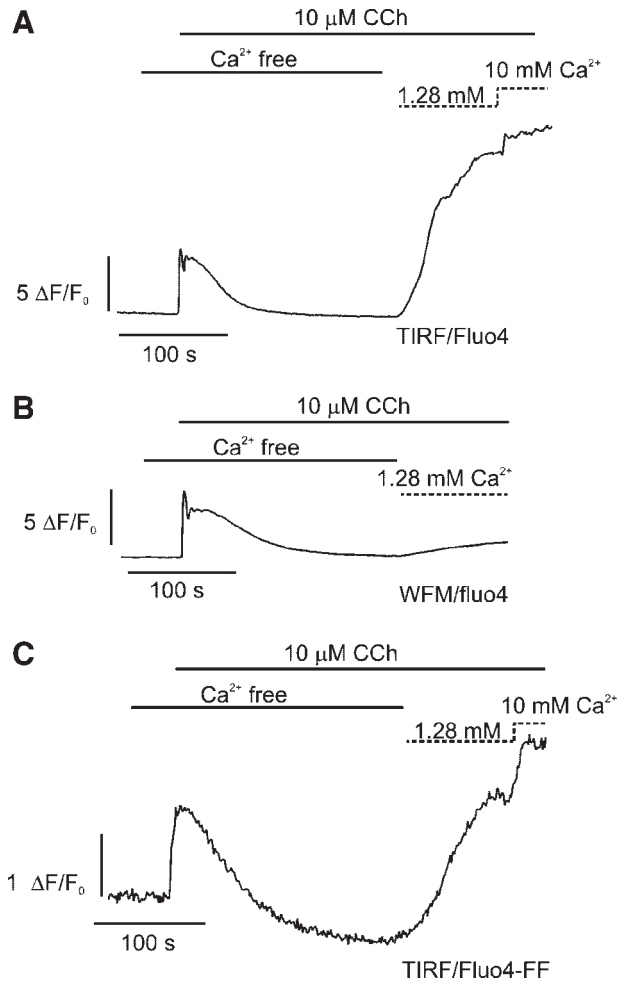

Fig. 5. Measurement of isolated Ca^{2+} release and Ca^{2+} influx in parotid acini using TIRFM and WFM. *A*: representative trace from a Fluo-4-loaded parotid acinus initially stimulated with a maximal concentration of CCh in the absence of extracellular Ca^{2+}. After the return of $[Ca^{2+}]_i$ to basal levels, extracellular Ca^{2+} was readmitted to the bathing media. The initial Ca^{2+} signal in the absence of extracellular Ca^{2+} as measured with TIRFM was not significantly different from that observed when measured with WFM (compare *A* and *B*). In contrast, the Ca^{2+} signal following readmission of extracellular Ca^{2+} was markedly greater when measured with TIRFM (compare *A* and *B*). When extracellular Ca^{2+} was raised to 10 mM, only a modest further increase in the signal occurred, presumably because the dye is close to saturation. *B*: a similar protocol to *A* is performed with WFM. *C*: a similar protocol to *A* is performed in cells loaded with the lower affinity indicator Fluo-4-FF. A more marked increase after raising extracellular Ca^{2+} to 10 mM is observed.

trigger for Ca^{2+} influx (15, 21, 32, 48). We next performed TIRFM experiments to investigate whether artificial store depletion with a SERCA pump inhibitor would also reveal substantial Ca^{2+} influx in parotid acinar cells. Small parotid acini were bathed in Ca^{2+}-free extracellular media and subsequently incubated with cyclopiazonic acid (CPA; 30 μM). After the depletion of the Ca^{2+} store, Ca^{2+} was readmitted to the bathing solution. When measured using TIRFM, as shown in Fig. 6*A*, CPA treatment resulted in an initial increase in intracellular Ca^{2+} of comparable magnitude to that reported for WFM (see Fig. 8*C* for summary). On readmission of extracellular Ca^{2+}, however, a substantial increase in the Ca^{2+} signal was observed that was comparable to the magnitude reached following maximal agonist stimulation [16.23 ± 2.77 ΔF units (n = 5); and see Figs. 5*A* and 8 for summary]. These data also serve to strengthen the contention that the large increase in $[Ca^{2+}]_i$ following extracellular Ca^{2+} readmission is not due to CICR, because these conditions obviously reflect the absence of functional Ca^{2+} stores. Again, the signal when measured with TIRFM in Fluo-4-loaded cells appeared saturated because increasing extracellular Ca^{2+} from 1.28 to 10 mM did not result in any further substantial increase in the fluorescence signal, whereas in Fluo-4-FF-loaded cells, the fluorescence increased following this maneuver (Fig. 6*B*). These data are again consistent with the ability of TIRFM with Fluo-4 to measure near saturated, subplasma membrane Ca^{2+} changes not apparent with WFM.

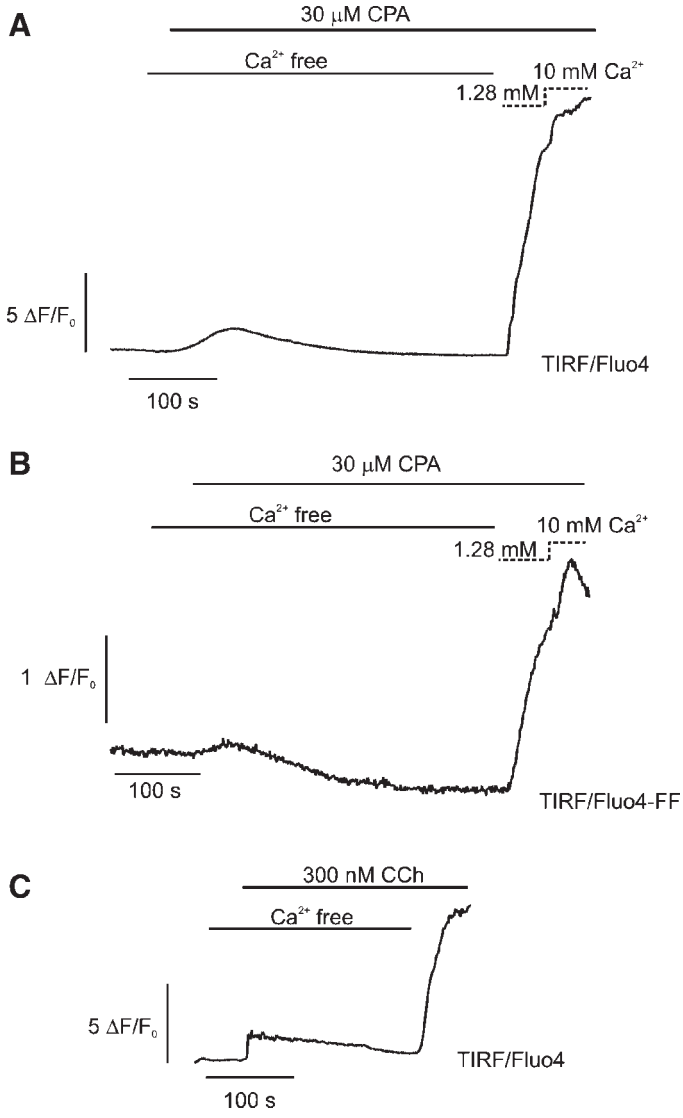

Fig. 6. TIRFM measurement following SERCA pump inhibition and stimulation with physiological concentrations of agonist in parotid acini. *A*: representative trace of a parotid acinus, loaded with Fluo-4 and incubated with cyclopiazonic acid (CPA), a SERCA pump inhibitor. In the absence of extracellular Ca^{2+}, only a modest increase in $[Ca^{2+}]_i$ was observed. Subsequent readmission of extracellular Ca^{2+} resulted in a robust Ca^{2+} signal that did not markedly increase when extracellular Ca^{2+} was increased to 10 mM. *B*: identical protocol was followed but using an acinus loaded with Fluo-4-FF. Elevating extracellular Ca^{2+} from 1.28 to 10 mM resulted in a further increase in the signal. *C*: Fluo-4-loaded parotid acinus was stimulated with a physiological concentration of CCh (300 nM) in the absence of extracellular Ca^{2+}. Readmission of extracellular Ca^{2+} resulted in a robust increase in $[Ca^{2+}]_i$.

At more physiological concentrations of agonist, only minimal store depletion is thought to occur; nevertheless, stimulation of exocrine cells is accompanied by significant Ca^{2+} entry, especially in parotid acinar cells (26). We, therefore, next investigated the extent of Ca^{2+} influx as measured with the Ca^{2+} readdition protocol with physiological concentrations of agonists. As shown in Fig. 6C, stimulation of parotid acini with 300 nM CCh in Ca^{2+}-free media resulted in the initiation of a Ca^{2+} signal that was often characterized by periodic oscillations when measured with TIRFM. When Ca^{2+} was readmitted to the bathing media, robust Ca^{2+} signals were observed, which reached levels far exceeding those attained in WFM mode, even at maximal concentrations of agonist as shown in Fig. 5*B*. These data indicate that TIRFM reveals Ca^{2+} entry of significant magnitude, not observed in WFM, even at physiological concentrations of agonists.

Measurement of isolated agonist-induced Ca^{2+} release and Ca^{2+} influx with TIRFM in pancreatic acini. Experiments were next performed to assess the extent of Ca^{2+} release and Ca^{2+} influx in pancreatic acinar cells using TIRFM and WFM. Initially, small acini were stimulated with maximal concentrations of agonists in the absence of extracellular Ca^{2+}, and then after the return of the Ca^{2+} signals to prestimulus levels, 1.28 mM Ca^{2+} was readmitted to the extracellular bathing media. As shown in Fig. 7, this protocol resulted in a rapid release of intracellular Ca^{2+} that was not significantly different when measured with either TIRFM [4.70 ± 0.33 ΔF units (n = 12); Fig. 7*A*] or WFM [4.20 ± 0.25 ΔF units (n = 3); Fig. 7*C* and summary in Fig. 8*A*; t-test $P > 0.05$]. The magnitude of this Ca^{2+} release in pancreatic acini, although less, was not significantly different from the values obtained for parotid acini when measured with TIRFM (4.7 ± 0.33 vs. 6.25 ± 0.35 ΔF units; pancreas vs. parotid, respectively; see Fig. 8 for summary). When Ca^{2+} was replaced in the extracellular bathing media, in a similar fashion to parotid acinar cells, the Ca^{2+} signal appeared significantly larger when measured with TIRFM vs. WFM [1.56 ± 0.21 (n = 12) vs. 0.44 ± 0.07 (n = 3) ΔF units, respectively, t-test $P < 0.01$]. However, compared with parotid, the magnitude of the Ca^{2+} increase was markedly less (see Fig. 8*A*; t-test $P < 0.01$). Indeed, in contrast to parotid acinar cells, where the signal appeared largely saturated, this was not the case in pancreatic acinar cells, because elevating external Ca^{2+} from 1.28 to 10 mM resulted in a significant further increase in the signal, confirming that the indicator was not saturated as shown in Fig. 7*A*. Similar

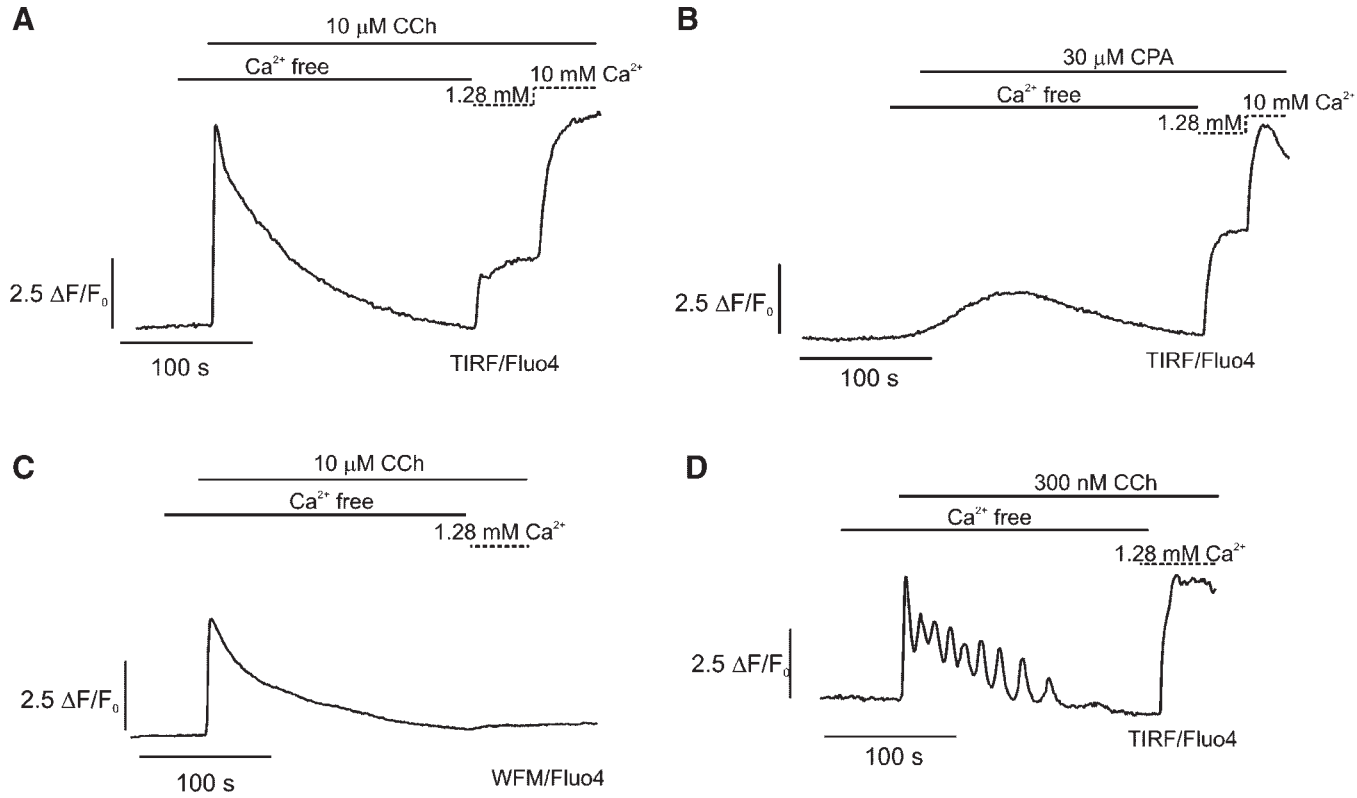

Fig. 7. Measurement of isolated Ca^{2+} release and Ca^{2+} influx in pancreatic acini using TIRFM and WFM. *A*: representative trace using TIRFM of a Fluo-4-loaded pancreatic acinus stimulated with a maximal concentration of agonist in the absence of extracellular Ca^{2+}. In contrast to experiments performed with WFM (see Fig. 6*C*), subsequent readmission of 1.28 mM extracellular Ca^{2+} resulted in a marked, rapid increase in the Ca^{2+} signal. Increasing extracellular Ca^{2+} to 10 mM, in contrast to experiments performed in parotid (see Fig. 4*A*), resulted in a substantial further increase in the signal indicating that the dye was not saturated. *B*: pancreatic acinus was treated with CPA in the absence of extracellular Ca^{2+} followed by readmission of extracellular Ca^{2+}. *C*: similar experimental paradigm as *A* but performed with WFM. *D*: pancreatic acinus was stimulated with a low concentration of CCh (300 nM) initially in the absence of extracellular Ca^{2+}. After the return of the Ca^{2+} signal to basal values, Ca^{2+} was readmitted to the extracellular media, resulting in a further increase in $[Ca^{2+}]_i$.

conclusions could be reached with experiments in which the Ca^{2+} stores were maximally depleted with CPA (30 μM). As shown in Fig. 7*B*, whereas the initial Ca^{2+} release measured with TIRFM was of comparable magnitude with that observed in parotid acinar cells [1.92 ± 0.2 (n = 4) vs. 1.45 ± 0.47 (n = 5) parotid vs. pancreas, respectively; t-test, $P > 0.05$], readdition of extracellular Ca^{2+} resulted in an increase in Ca^{2+} signal, which was significantly reduced when compared with the magnitude in parotid acinar cells [3.37 ± 0.47 (n = 5) vs. 16.23 + 2.77 (n = 4) ΔF units, pancreas vs. parotid, respectively; and see Fig. 8*C* for summary, t-test $P < 0.01$].

Next, experiments were performed stimulating pancreatic acinar cells with more physiological concentrations of agonist in the absence and presence of extracellular Ca^{2+}. As shown in Fig. 7*D*, stimulation with 300 nM CCh resulted in the initiation of Ca^{2+} oscillations, which, in the absence of extracellular Ca^{2+}, were not maintained. Subsequent readdition of Ca^{2+} to the extracellular media resulted in a modest increase in the Ca^{2+} signal, which, in a similar fashion to maximal concentrations of agonist, was significantly smaller in pancreatic acini compared with acini prepared from parotid gland [2.3 ± 2.9 (n = 6) vs. 10.8 ± 0.93 (n = 15) ΔF units, pancreas vs. parotid, respectively; t-test $P < 0.01$; and see Fig. 8*B* for summary]. These data indicate that after maximal or physiological agonist stimulation, or after store depletion in pancreatic acinar cells, TIRFM is more effective than WFM at detecting Ca^{2+} signals as a result of Ca^{2+} influx, although these signals are much smaller than those seen in parotid acinar cells.

DISCUSSION

A great deal of information regarding the spatial and temporal characteristics of Ca^{2+}-signaling dynamics has been gained by WF or confocal imaging studies of exocrine acinar cells. However, whereas much important information has been reported, these studies are potentially limited by spatial resolution, especially in the z dimension. A lack of spatial resolution would tend to underestimate the magnitude of Ca^{2+} signals as the signals are globally averaged. This is especially applicable to signals that originate at the plasma membrane. Indeed, with the use of genetically targeted plasma membrane probes, it has been elegantly demonstrated both in electrically excitable and in nonexcitable systems that global measurements grossly underestimate the magnitude of subplasma membrane Ca^{2+} signals (22, 23). This drawback of WFM may be of particular relevance in exocrine cells where both the initiation of Ca^{2+} release through Ins(1,4,5)P_3R and the maintenance of the Ca^{2+} signal through Ca^{2+} influx occur in a restricted area often at, or very close to, the plasma membrane. Although terminally differentiated, acutely isolated exocrine acinar cells are not readily amenable to expression of spatially localized, genetically targeted indicators; an alternative solu-

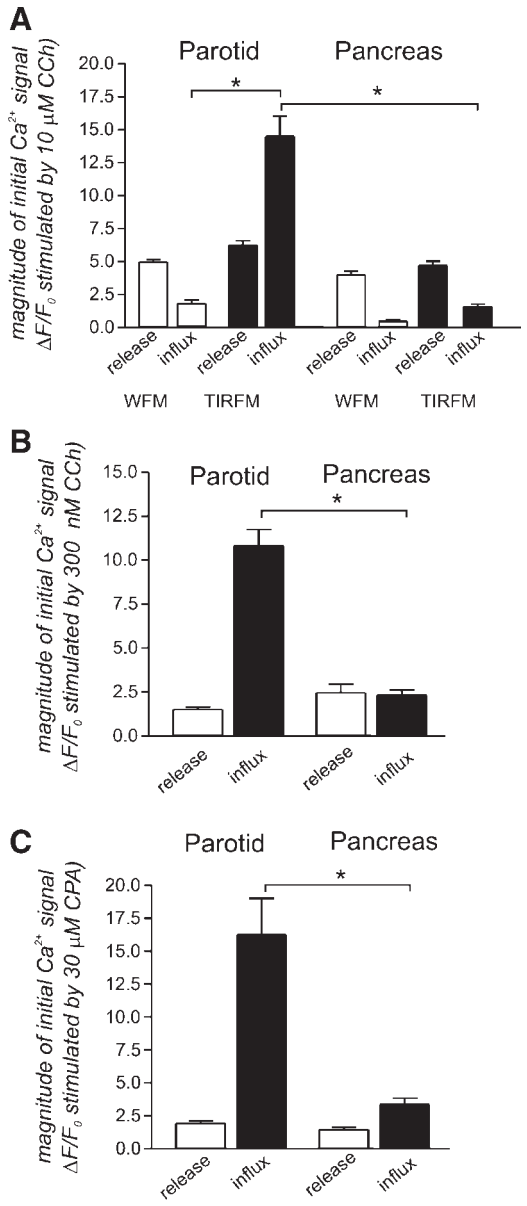

Fig. 8. *A*: magnitude of the initial signal stimulated by 10 μM CCh initially in the absence of extracellular Ca^{2+} and subsequently following readmission of Ca^{2+} to the bathing media for both pancreatic and parotid acini measured with both WFM and TIRFM. No significant differences were observed comparing the initial Ca^{2+} release measured with WFM vs. TIRFM . In both cell types, the magnitude of the signal following Ca^{2+} readmission to the extracellular solution was significantly larger when measured with TIRFM vs. WFM (nonpaired *t*-test, $P < 0.01$, for both cell types). In addition, this signal was significantly larger in parotid compared with pancreatic acinar cells (nonpaired *t*-test, $P < 0.01$). *B*: magnitude of the initial signal stimulated by 300 nM CCh and measured with TIRFM, initially in the absence of extracellular Ca^{2+} and subsequently following readmission of Ca^{2+} to the bathing media for both pancreatic and parotid acini. The magnitude of the signal following readmission of Ca^{2+} to the extracellular media is significantly larger in parotid compared with pancreatic acini (*t*-test, $P < 0.01$). *C*: magnitude of the initial signal stimulated by 30 μM CPA initially in the absence of extracellular Ca^{2+} and subsequently following readmission of Ca^{2+} to the bathing media for both pancreatic and parotid acini. The Ca^{2+} signal following Ca^{2+} readmission to the extracellular media was significantly larger when measured in parotid vs. pancreatic acinar cells (nonpaired *t*-test, $P < 0.01$).

tion to measure highly localized signals at the plasma membrane is to image only the indicator in this region. In this study, we have used TIRFM to image Ca^{2+} signals in exocrine acinar cells in a region restricted by the physical properties of the methodology to ~150–200 nm below the plasma membrane.

Initially, we designed experiments using TIRFM to monitor Ca^{2+} signals stimulated by physiological concentrations of agonist, which, in WFM, are typically manifested as Ca^{2+} oscillations. These oscillatory signals are primarily the result of cycles of Ins(1,4,5)P_3-mediated Ca^{2+} release followed by clearance via Ca^{2+} extrusion across the plasma membrane and sequestration into the endoplasmic reticulum and mitochondria. Nevertheless, Ca^{2+} influx is absolutely required to maintain the Ca^{2+} oscillations (46). In both parotid and pancreatic acinar cells using TIRFM, the Ca^{2+} signals stimulated by physiological concentrations of muscarinic agonists were not markedly different from those reported for WFM. Interestingly, the signals did not reflect obvious saturation of the indicator, which would be expected if monitoring Ca^{2+} in the close vicinity of the channels. Therefore, whereas TIRFM measurements under these conditions reflect local, agonist-stimulated subplasma membrane $[Ca^{2+}]_i$ elevations, the implication is that they actually only provide a local reflection of the global signal by monitoring diffusion primarily from distant intracellular Ca^{2+}-release sites. This is not entirely unexpected with respect to the measurement of Ca^{2+} release given the region in exocrine acinar cells that we show is subjected to TIRFM (Fig. 1) and that Ca^{2+} release is known to occur preferentially in the extreme apical pole of the cell (17, 18, 27, 35, 39). Therefore, these data reflect a limitation of this technique in cell types with complex three-dimensional architectures because excitation of the probe by the evanescent wave only occurs at the plasma membrane-coverglass interface and thus only at areas of contact.

Possibly more surprising is that the characteristics of the Ca^{2+} signal with TIRFM were largely similar to WFM considering the robust activity of Ca^{2+}-selective conductances known to be stimulated at these physiological concentrations of agonist (26). Again, Fluo-4 would be expected to be largely saturated in the vicinity of uniformly distributed Ca^{2+} influx channels. Indeed, this idea is supported by imaging of Ca^{2+} ionophore-stimulated Ca^{2+} elevations, which reflect the uniform transport of Ca^{2+} across the plasma membrane and appeared largely saturated (Fig. 3*C*). One possible explanation for this observation is that Ca^{2+} influx occurring at these physiological concentrations of agonist is not of sufficient magnitude to overcome local Ca^{2+} buffering and clearance. Support for this idea is offered by reports in T lymphocytes that sequestration of Ca^{2+} by mitochondria and pumping by PMCA (plasma membrane Ca^{2+}-ATPase) can markedly influence the activity of CRAC (Ca^{2+} release activated channels) channels (4, 16). In support of this idea, a subpopulation of mitochondria is localized to the plasma membrane in both parotid and pancreatic acinar cells (9, 31).

An alternative hypothesis to explain the apparent lack of influence of Ca^{2+} influx on these measurements is the possibility that, similar to Ca^{2+} release, Ca^{2+} influx stimulated at physiological concentrations of agonist does not occur uniformly across the plasma membrane. Localized influx could potentially occur by the local generation of messengers required to gate Ca^{2+} influx or through localized channels

mediating the Ca^{2+} influx. Given the localization of Ins(1,4,5)P_3R in exocrine acinar cells, a mechanism involving conformational coupling (5) of Ins(1,4,5)P_3R to Ca^{2+} influx channels primarily localized to the apical plasma membrane is attractive and would be consistent with the inability of TIRFM to measure substantial Ca^{2+} influx under these conditions.

Stimulation with supramaximal concentrations of agonist resulted in Ca^{2+} signals monitored by TIRFM with qualitatively similar characteristics to WFM, although we noted that the magnitude of the sustained plateau phase of indicative Ca^{2+} influx was greater than that reported for WFM. The contribution of Ca^{2+} influx under conditions of maximal stimulation was therefore investigated by isolating Ca^{2+} influx and release using a calcium readmission protocol, either following maximal agonist stimulation or store depletion following SERCA pump inhibition. This protocol is commonly used to monitor maximal Ca^{2+} release in the absence of extracellular Ca^{2+} followed by subsequent store depletion-gated Ca^{2+} influx as Ca^{2+} is readmitted to the extracellular bathing media. Experiments using TIRFM presented a number of novel observations, including the assessment of the magnitude of Ca^{2+} release and influx following substantial store depletion in each cell type and also importantly facilitated a comparison of the relative magnitude of these components in the two cell types. First, only minor differences in the magnitude of Ca^{2+} release following agonist stimulation were seen comparing TIRFM with WFM measurements in either cell type, again supporting the notion that Ca^{2+} release even at maximal stimulation is occurring at a point significantly distal to the areas subjected to TIRFM. In contrast, whereas only minor Ca^{2+} influx was observed following Ca^{2+} readmission in parotid acinar cells with WFM (Fig. 5), TIRFM revealed levels of $[Ca^{2+}]_i$, which largely saturated the high-affinity dye Fluo-4 in the area immediately below the plasma membrane (Fig. 5). Similar substantial increases in $[Ca^{2+}]_i$ using this protocol were also observed with TIRFM following inhibition of SERCA pumps and at physiological concentrations of agonists. The latter observation may reflect the fact that this protocol, unlike stimulation in the presence of extracellular Ca^{2+}, results in significant store depletion. These data indicate clearly that the magnitude of store depletion-gated Ca^{2+} entry is readily detectable using this experimental protocol only with TIRFM and, presumably, reflects the fact that Ca^{2+} influx following substantial store depletion appears to be occurring either into the volume of dye excited by the evanescent wave or very close to it.

Similarly, in pancreatic acinar cells subjected to an identical experimental protocol, the extent of the Ca^{2+} signal following Ca^{2+} readmission was substantially greater when measured with TIRFM than with WFM. However, the fluorescence change as a result of Ca^{2+} influx measured at the TIRFM sites was on average only ~10% that observed in parotid acinar cells. Whereas it is possible this might reflect differing localization of channels or buffering in pancreas compared with parotid, a parsimonious explanation for the apparent reduced relative magnitude of the Ca^{2+} influx in pancreas is the decreased expression of Ca^{2+}-conducting channels activated by this paradigm. This idea is consistent with a recent electrophysiological study that demonstrated substantially more Ca^{2+} conductance in parotid acinar cells compared with pancreatic acinar cells (26).

It is tempting to speculate that the apparent differing magnitudes of Ca^{2+} influx in parotid and pancreatic acinar cells are important in the specialized physiology of the individual cell types. Pancreatic acinar cells principally secrete zymogen granules by exocytosis at the apical pole of the cell. The localization of Ins(1,4,5)P_3R in the apical pole appears to be ideally situated to provide the Ca^{2+} requirement for exocytosis. In the case of pancreatic acinar cells, the requirement for Ca^{2+} influx for secretion may simply be to replenish the intracellular Ca^{2+} stores. The primary role of parotid gland acinar cells is to produce primary saliva, which is accomplished in a Ca^{2+}-dependent manner by the activation of plasma membrane ion channels that are proposed to be spatially separated on the apical and basolateral aspects of the cell (25). That Ca^{2+} influx is required for optimal fluid secretion has long been known, because sustained ion-channel activation and fluid secretion absolutely require Ca^{2+} influx in salivary glands (24, 29). Furthermore, it has been shown that adenoviral overexpression of TRPC1, a candidate protein proposed to mediate store depletion-gated Ca^{2+} influx in salivary glands, results in markedly increased saliva production in mice (34). Whereas it is possible that Ca^{2+} influx is simply required under these conditions to maintain intracellular Ca^{2+} pools, it is, nevertheless, a possibility that robust spatially uniform Ca^{2+} signals at the plasma membrane as a result of substantial Ca^{2+} influx in salivary acinar cells are required for efficient direct activation of ion channels and, ultimately, fluid secretion from the gland.

ACKNOWLEDGMENTS

The authors thank T. Shuttleworth, M. Betzenhauser, D. Brown, and L. Wagner for helpful discussion throughout the study.

GRANTS

The work was supported by NIH Grants R01-DK-54568, R01-DE-14756, and R01-DE-16999.

REFERENCES

1. **Ambudkar IS.** Regulation of calcium in salivary gland secretion. *Crit Rev Oral Biol Med* 11: 4–25, 2000.
2. **Ashby MC and Tepikin AV.** Polarized calcium and calmodulin signaling in secretory epithelia. *Physiol Rev* 82: 701–734, 2002.
3. **Axelrod D.** Total internal reflection fluorescence microscopy in cell biology. *Methods Enzymol* 361: 1–33, 2003.
4. **Bautista DM and Lewis RS.** Modulation of plasma membrane calcium-ATPase activity by local calcium microdomains near CRAC channels in human T cells. *J Physiol* 556: 805–817, 2004.
5. **Berridge MJ.** Capacitative calcium entry. *Biochem J* 312: 1–11, 1995.
6. **Berridge MJ, Lipp P, and Bootman MD.** The versatility and universality of calcium signalling. *Nat Rev Mol Cell Biol* 1: 11–21, 2000.
7. **Betz WJ, Mao F, and Smith CB.** Imaging exocytosis and endocytosis. *Curr Opin Neurobiol* 6: 365–371, 1996.
8. **Bruce JI, Shuttleworth TJ, Giovannucci DR, and Yule DI.** Phosphorylation of inositol 1,4,5-trisphosphate receptors in parotid acinar cells. A mechanism for the synergistic effects of cAMP on Ca^{2+} signaling. *J Biol Chem* 277: 1340–1348, 2002.
9. **Bruce JI, Giovannucci DR, Blinder G, Shuttleworth TJ, and Yule DI.** Modulation of $[Ca^{2+}]_i$ signaling dynamics and metabolism by perinuclear mitochondria in mouse parotid acinar cells. *J Biol Chem* 279: 12909–12917, 2004.
10. **Demuro A and Parker I.** Imaging the activity and localization of single voltage-gated Ca^{2+} channels by total internal reflection fluorescence microscopy. *Biophys J* 86: 3250–3259, 2004.
11. **Demuro A and Parker I.** Optical single-channel recording: imaging Ca^{2+} flux through individual ion channels with high temporal and spatial resolution. *J Biomed Opt* 10: 11002, 2005.

12. **Evans RL, Bell SM, Schultheis PJ, Shull GE, and Melvin JE.** Targeted disruption of the Nhe1 gene prevents muscarinic agonist-induced up-regulation of Na(+)/H(+) exchange in mouse parotid acinar cells. *J Biol Chem* 274: 29025–29030, 1999.
13. **Fogarty KE, Kidd JF, Tuft DA, and Thorn P.** Mechanisms underlying InsP3-evoked global Ca^{2+} signals in mouse pancreatic acinar cells. *J Physiol* 526: 515–526, 2000.
14. **Giovannucci DR, Bruce JI, Straub SV, Arreola J, Sneyd J, Shuttleworth TJ, and Yule DI.** Cytosolic Ca^{2+} and Ca^{2+}-activated Cl^- current dynamics: insights from two functionally distinct mouse exocrine cells. *J Physiol* 540: 469–484, 2002.
15. **Hoth M and Penner R.** Depletion of intracellular calcium stores activates a calcium current in mast cells. *Nature* 355: 353–356, 1992.
16. **Hoth M, Fanger CM, and Lewis RS.** Mitochondrial regulation of store-operated calcium signaling in T lymphocytes. *J Cell Biol* 137: 633–648, 1997.
17. **Kasai H and Augustine GJ.** Cytosolic Ca^{2+} gradients triggering unidirectional fluid secretion from exocrine pancreas. *Nature* 348: 735–738, 1990.
18. **Kasai H, Li YX, and Miyashita Y.** Subcellular distribution of Ca^{2+} release channels underlying Ca2+ waves and oscillations in exocrine pancreas. *Cell* 74: 669–677, 1993.
19. **Lee MG, Xu X, Zeng W, Diaz J, Kuo TH, Wuytack F, Racymaekers L, and Muallem S.** Polarized expression of Ca^{2+} pumps in pancreatic and salivary gland cells. Role in initiation and propagation of $[Ca^{2+}]_i$ waves. *J Biol Chem* 272: 15771–15776, 1997.
20. **Lee MG, Xu X, Zeng W, Diaz J, Wojcikiewicz RJ, Kuo TH, Wuytack F, Racymaekers L, and Muallem S.** Polarized expression of Ca^{2+} channels in pancreatic and salivary gland cells. Correlation with initiation and propagation of $[Ca^{2+}]_i$ waves. *J Biol Chem* 272: 15765–15770, 1997.
21. **Liu X and Ambudkar IS.** Characteristics of a store-operated calcium-permeable channel: sarcoendoplasmic reticulum calcium pump function controls channel gating. *J Biol Chem* 276: 29891–29898, 2001.
22. **Llinas R, Sugimori M, and Silver RB.** Microdomains of high calcium concentration in a presynaptic terminal. *Science* 256: 677–679, 1992.
23. **Marsault R, Murgia M, Pozzan T, and Rizzuto R.** Domains of high Ca^{2+} beneath the plasma membrane of living A7r5 cells. *EMBO J* 16: 1575–1581, 1997.
24. **Melvin JE, Koek L, and Zhang GH.** A capacitative Ca2+ influx is required for sustained fluid secretion in sublingual mucous acini. *Am J Physiol Gastrointest Liver Physiol* 261: G1043–G1050, 1991.
25. **Melvin JE, Yule D, Shuttleworth T, and Begenisich T.** Regulation of fluid and electrolyte secretion in salivary gland acinar cells. *Annu Rev Physiol* 67: 445–469, 2005.
26. **Mignen O, Thompson JL, Yule DI, and Shuttleworth TJ.** Agonist activation of arachidonate-regulated Ca2+-selective (ARC) channels in murine parotid and pancreatic acinar cells. *J Physiol* 564: 791–801, 2005.
27. **Nathanson MH, Padfield PJ, O'Sullivan AJ, Burgstahler AD, and Jamieson JD.** Mechanism of Ca^{2+} wave propagation in pancreatic acinar cells. *J Biol Chem* 267: 18118–18121, 1992.
28. **Nathanson MH, Fallon MB, Padfield PJ, and Maranto AR.** Localization of the type 3 inositol 1,4,5-trisphosphate receptor in the Ca^{2+} wave trigger zone of pancreatic acinar cells. *J Biol Chem* 269: 4693–4696, 1994.
29. **Nauntofte B and Poulsen JH.** Effects of Ca2+ and furosemide on Cl^- transport and O2 uptake in rat parotid acini. *Am J Physiol Cell Physiol* 251: C175–C185, 1986.
30. **Nezu A, Tanimura A, Morita T, Irie K, Yajima T, and Tojyo Y.** Evidence that zymogen granules do not function as an intracellular Ca^{2+} store for the generation of the Ca^{2+} signal in rat parotid acinar cells. *Biochem J* 363: 59–66, 2002.
31. **Park MK, Ashby MC, Erdemli G, Petersen OH, and Tepikin AV.** Perinuclear, perigranular and sub-plasmalemmal mitochondria have distinct functions in the regulation of cellular calcium transport. *EMBO J* 20: 1863–1874, 2001.
32. **Putney JW Jr.** A model for receptor-regulated calcium entry. *Cell Calcium* 7: 1–12, 1986.
33. **Schneckenburger H.** Total internal reflection fluorescence microscopy: technical innovations and novel applications. *Curr Opin Biotechnol* 16: 13–18, 2005.
34. **Singh BB, Zheng C, Liu X, Lockwich T, Liao D, Zhu MX, Birnbaumer L, and Ambudkar IS.** Trp1-dependent enhancement of salivary gland fluid secretion: role of store-operated calcium entry. *FASEB J* 15: 1652–1654, 2001.
35. **Straub SV, Giovannucci DR, and Yule DI.** Calcium wave propagation in pancreatic acinar cells: functional interaction of inositol 1,4,5-trisphosphate receptors, ryanodine receptors, and mitochondria. *J Gen Physiol* 116: 547–560, 2000.
36. **Stuenkel EL, Tsunoda Y, and Williams JA.** Secretagogue induced calcium mobilization in single pancreatic acinar cells. *Biochem Biophys Res Commun* 158: 863–869, 1989.
37. **Takemura H and Putney JW Jr.** Capacitative calcium entry in parotid acinar cells. *Biochem J* 258: 409–412, 1989.
38. **Thomas D, Tovey SC, Collins TJ, Bootman MD, Berridge MJ, and Lipp P.** A comparison of fluorescent Ca^{2+} indicator properties and their use in measuring elementary and global Ca2+ signals. *Cell Calcium* 28: 213–223, 2000.
39. **Thorn P, Lawrie AM, Smith PM, Gallacher DV, and Petersen OH.** Local and global cytosolic Ca^{2+} oscillations in exocrine cells evoked by agonists and inositol trisphosphate. *Cell* 74: 661–668, 1993.
40. **Tinel H, Cancela JM, Mogami H, Gerasimenko JV, Gerasimenko OV, Tepikin AV, and Petersen OH.** Active mitochondria surrounding the pancreatic acinar granule region prevent spreading of inositol trisphosphate-evoked local cytosolic Ca^{2+} signals. *EMBO J* 18: 4999–5008, 1999.
41. **Tsunoda Y, Stuenkel EL, and Williams JA.** Characterization of sustained $[Ca^{2+}]_i$ increase in pancreatic acinar cells and its relation to amylase secretion. *Am J Physiol Gastrointest Liver Physiol* 259: G792–G801, 1990.
42. **Tsunoda Y, Stuenkel EL, and Williams JA.** Oscillatory mode of calcium signaling in rat pancreatic acinar cells. *Am J Physiol Cell Physiol* 258: C147–C155, 1990.
43. **Williams JA, Korc M, and Dormer RL.** Action of secretagogues on a new preparation of functionally intact, isolated pancreatic acini. *Am J Physiol* 235: 517–524, 1978.
44. **Williams JA, Groblewski GE, Ohnishi H, and Yule DI.** Stimulus-secretion coupling of pancreatic digestive enzyme secretion. *Digestion* 58, *Suppl* 1: 42–45, 1997.
45. **Yao J, Li Q, Chen J, and Muallem S.** Subpopulation of store-operated Ca^{2+} channels regulate Ca^{2+}-induced Ca^{2+} release in non-excitable cells. *J Biol Chem* 279: 21511–21519, 2004.
46. **Yule DI and Gallacher DV.** Oscillations of cytosolic calcium in single pancreatic acinar cells stimulated by acetylcholine. *FEBS Lett* 239: 358–362, 1988.
47. **Yule DI, Ernst SA, Ohnishi H, and Wojcikiewicz RJ.** Evidence that zymogen granules are not a physiologically relevant calcium pool. Defining the distribution of inositol 1,4,5-trisphosphate receptors in pancreatic acinar cells. *J Biol Chem* 272: 9093–9098, 1997.
48. **Zweifach A and Lewis RS.** Mitogen-regulated Ca^{2+} current of T lymphocytes is activated by depletion of intracellular Ca^{2+} stores. *Proc Natl Acad Sci USA* 90: 6295–6299, 1993.